Lux junior 2024

17. Internationales Forum für den lichttechnischen Nachwuchs
Ilmenau, 6. – 8. September 2024
DOI (proceedings): 10.22032/dbt.61636

DOI: 10.22032/dbt.xxxxx

Investigation on the influence and uncertainty contribution of the photometric center on photogoniometric measurements

M.Sc. Leonhard Klaus Dudzik, Dr. Klaus Trampert, Prof. Dr. rer. nat. Cornelius Neumann, Karlsruhe Institute of Technology – Light Technology Institute

Abstract

How much light an object emits in certain directions is described by its Luminous Intensity Distribution (LID). It results from integrating over the Luminance of all emitting surfaces, thereby implicitly modelling the object as a point source. The point of the object, that best describes it as a point source, is called the Photometric Center. It is the origin of a source coordinate system, that the LID is expressed in. A far field measurement setup defines its own coordinate system, that has to coincide with the source's coordinate system. If the Photometric Center and machine center are misaligned the LID measurement is distorted.

This paper proposes a model for common far field goniometer geometries and sources that allows to quantify the effect the source position has on the resulting LID. Since the photometric center can only be estimated with a limited confidence, it contributes to the uncertainty of the LID measurement. Therefore, Monte Carlo Simulation is utilized to quantify this uncertainty contribution and determine the conditions, where it becomes significant.

1 Luminous Intensity Distribution Measurements

Luminous Intensity (I) is a measure for the amount of light emitted in a certain solid angle or direction and has the unit candela (cd). It is derived by integrating over the Luminance L for all surfaces of an object or region for one direction. Luminous Intensity can be understood as a simplified model of a luminous region: All light is assumed to originate from the same location, thereby representing the region as a point – called the Photometric Center (PC). This brings a welcome reduction in dimensionality, since Luminous Intensity is for many applications sufficient to describe the luminous properties of an object. Where the PC lies for a certain region, and what impact neglecting it has on photometric measurements of I, is discussed in depth in the following chapters.

Luminous Intensity is measured using Illuminance-detectors. It is inferred from an Illuminance measurement using the Photometric Distance Law (1.1) solved for I.

$$E = \frac{I}{r^2} \cdot cos(\alpha) \tag{1.1}$$

It states that a point source generates an Illuminance on a surface according to its Luminous Intensity in that direction, which is inversely proportional to the squared distance from the source. If the surface is not illuminated perpendicularly, the Illuminance is calculated for the apparent surface, using the incidence angle α.

A measurement setup for Luminous Intensity consists of an Illuminance detector and a known measurement geometry described by r and α. This principle is used in far field gonio-photometry, which deals with the measurement of Luminous Intensity for many directions, often on a dense angular grid. The concatenation of these measurements is called Luminous Intensity Distribution (LID).

1.1 The Photometric Center (PC)

In the EN 13032-1 norm for photometric measurements [1] the PC is defined as the point for which the Photometric Distance Law (1.1) is applicable. For finite distances the Illuminance produced by a three-dimensional object deviates from the value predicted by this law for a point source with the object's LID, converging for infinite distance. The PC is the location, that minimizes this difference.

This definition is not very helpful for determining the PC. Said norm offers examples and rules on how to estimate the PC for certain cases. For many objects however, finding its PC is not trivial. The PC is not confined to the region, where the emission is generated, since any optical elements alter its location.

The PC can be calculated, if there is Luminance information available for the luminaire, for example in the form of ray data from a near field goniometer measurement [2]. The PC is then the weighted center of the rays. This information is not available in most cases, since it would make the far field measurement unnecessary.

Another way to determine the PC is by extrapolating the location from multiple Illuminance measurements taken from different distances using the Photometric Distance Law. This is suitable for measurements of Luminous Intensity for a single direction on an optical bench. While multiple distances could be realized for every direction of a far field measurement, it would greatly increase its complexity and duration.

1.2 Coordinate Systems

Because of the point source assumption inherent to a LID, its directions are expressed relative to this point, the PC in a spherical coordinate system. There are different conventions as to how to define the polar and azimuth angle used to describe a direction. For the scope of this analysis the prevalent C-plane system described in the EN13032-1 norm [1] is used for the so-called the source coordinate system. It defines the Luminous Intensity directions inside a pencil of planes constructed along the azimuth angle as pictured in Figure 1.

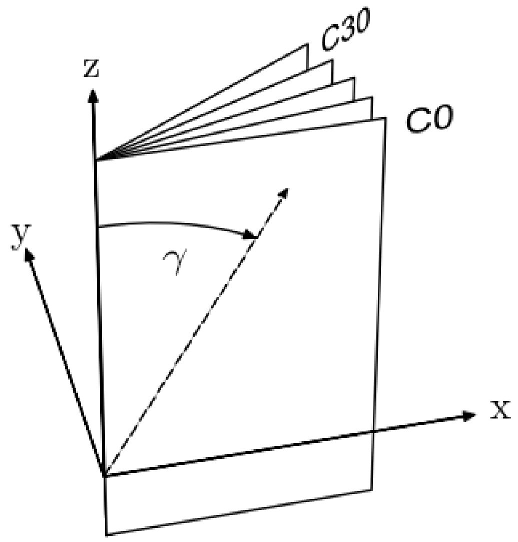

Figure 1 source coordinate system

The azimuth angle C is used for indexing the planes, starting at the x-axis. A direction lying within one of the planes is defined by the polar angle γ, as indicated on the C0 plane. The naming convention for the cartesian axes is different from the norm. The $\mathrm{x}, \mathrm{y}, \mathrm{z}$ axes correspond to the second, third and first axis respectively.

A far field goniometer works by either moving an Illuminance detector around the object or the object relative to the detector. Either way the rotation axes of the goniometer define a spherical coordinate system, that is shown in Figure 2. The polar and azimuth angles are denoted with θ and φ respectively and describe the orientation of the axes and consequently also that of the detector. There is normally no distinction between the machine and source coordinate system. It is assumed that the light is coming from the rotation origin of the machine coordinate system and both coordinate systems therefore coincide. They are treated separately here to be able to model a misaligned source.

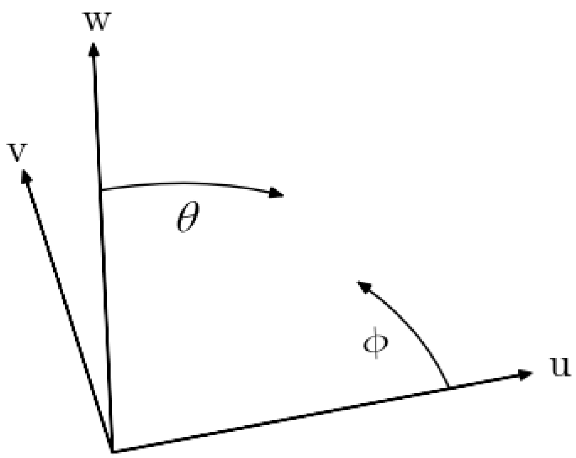

Figure 2 machine coordinate system

2 Geometric Challenges of Far field Photogoniometry

The challenges described in this section only apply for LID measurements. A Luminous Flux measurement performed with a goniometer is unaffected by the Limiting Photometric Distance and source alignment. This is because it is calculated as the integral of the Illuminance on a sphere, which is invariant.

2.1 Limiting Photometric Distance

A far field LID measurement is only an approximation, since the Photometric Distance Law is only exact for point sources, which are a mathematical construct not possible in reality. The light that the detector receives from different parts of the object are emitted under different angles but attributed to a single direction, resulting in a measurement error. The discrepancy between the observed angles and therefore the error decreases for higher measurement distances. How great the distance needs to be in order to reduce the deviation to an accepted amount has been explored under the topic of the Limiting Photometric Distance [3]. Without Luminance information for an object, the measurement deviation caused by the finite measurement distance can neither be estimated nor corrected. Instead rules are used to estimate the necessary distance as a factor of the objects largest dimension.

2.2 Alignment of the machine and source coordinate system

Most goniometers are constructed so that the geometry between source and detector is constant: The detector stays in a distance r around the rotation center with a constant tilt α towards the center. A Luminous Intensity measurement is then reported according to equation (2.1).

$$I_m(C,\gamma) \stackrel{\text{def}}{=} I_m(\phi,\theta) = E(\phi,\theta) \cdot \frac{r^2}{cos(\alpha)} \tag{2.1}$$

The Illuminance on the detector is sampled for a machine direction (ϕ, θ). The factor used to convert Illuminance to the measured Luminous Intensity I_m is derived from the assumed centered geometry and used for every measurement. The result is assigned to the source coordinate system, equating the spherical coordinates.

A case where the source is not positioned and oriented correctly is shown in Figure 3. It shows a two-dimensional representation of the machine coordinate system with a translated and rotated source placed inside.

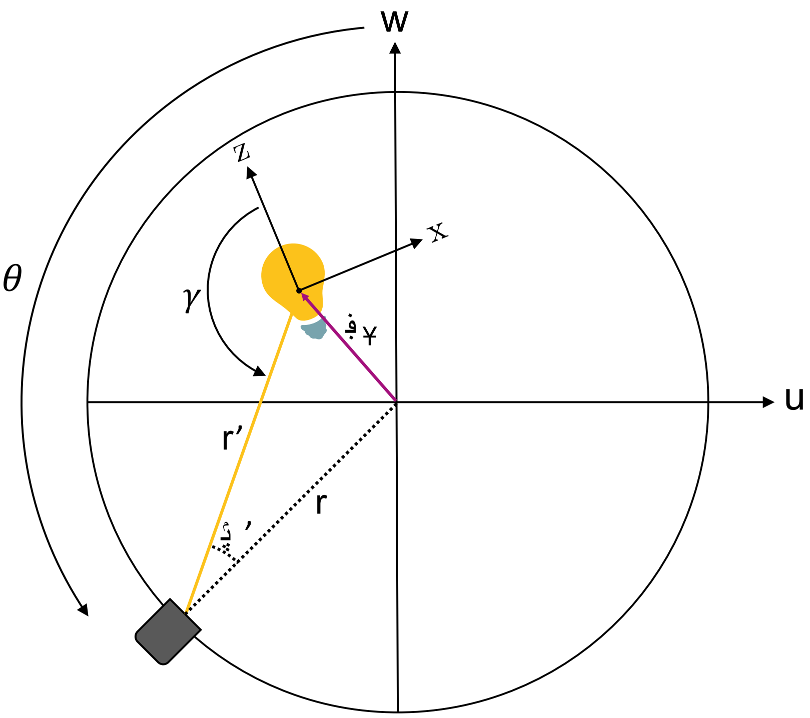

Figure 3 geometry of a misaligned source

With the source offset from the machine center by the vector $\mathbf{s_m}$, the assumed geometry is no longer valid. The distance between source and detector is changed from r to r'. Also, the incidence angle, with which the light hits the detector is changed. With the goniometer moved to a certain direction given by ϕ, θ the LID of the source is sampled at diverging angles C, γ. The LID is nonetheless calculated from the illuminance according to equation (2.1) assuming the centred geometry, which results in a measurement error.

The rotation of the object in the source coordinate system is dictated by the measurement procedure. It is aligned either to features of the LID or some mechanical reference of the object. Changes in rotation map 1:1 to the LID measurement [4]. The result is a coordinate shift of the LID, a constant offset between the angles ϕ and C or θ and γ. As long as the region of interest is inside the sampled solid angle, there is no loss of information and the orientation can be corrected after the measurement by aligning the coordinate system to feature a of the LID – for instance the maximum Luminous Intensity or the light-dark cut-off for headlamps. It is also possible to estimate and correct the rotation between two LIDs via correlation [5].

The geometry shown in Figure 3 is only applicable for this detector position. Since the detector rotates around the machine center, a translation between the coordinate systems creates a unique constellation between source and detector for every measurement direction. This results in a distortion of the LID. An example of this is shown in Figure 4.

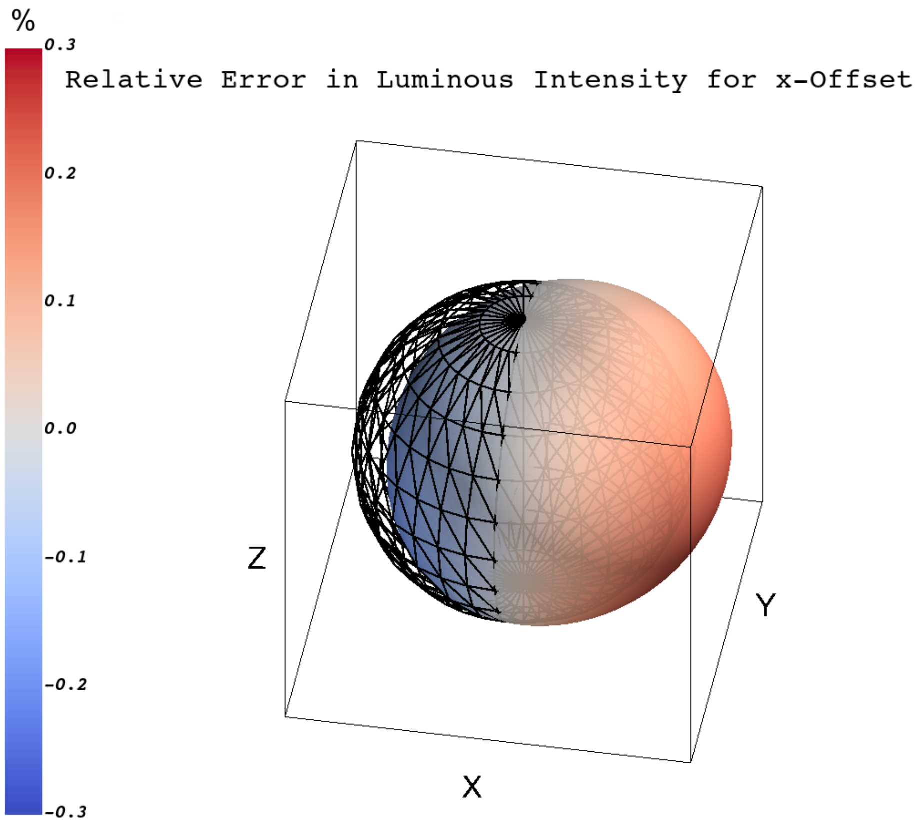

Figure 4 Distortion of a LID measurement for a Lambertian source

It depicts a simulated measurement of a Lambertian source with a displacement along the x-Axis by 0.1% of the measurement distance. The original LID of the Lambertian source is drawn as a wire mesh and the “measured” erroneous LID is coloured to express the relative deviation to the original source LID. As can be seen in Figure 4 Certain regions of the LID are increased, while others are decreased. The extent of this deviation is enlarged in the figure for better visibility. Because the deviation changes smoothly over directions, it is impossible to detect or separate this influence without prior knowledge of the LID. The impact of the translation is well below 1% for this example. Section 4 explores situations with a more serious impact.

3 Model of a Goniometer measurement with a translated Photometric Center

A model of a far field goniometer is created, that allows investigating the influence of the PC without the need to do countless measurements. The model is a simplified representation of a far field goniometer and a translated source inside it. The goal of the model is to calculate the measured pseudo LID $I_m(\mathrm{C},\gamma)$ for a given goniometer geometry, LID of the source $I_s(\mathrm{C},\gamma)$ and translation vector $\mathbf{s_m} = (\mathrm{s_u}, \mathrm{s_v}, \mathrm{s_w})$ of the source in machine coordinates.

To isolate the influence of the PC, every other aspect of photometry is treated as ideal. The detector has no size, the geometry of the goniometer is assumed to be known exactly. The source is modelled as a point source, which is justified if the measurement distance is great enough, so that the error from the source's size is negligible. Further the model does not include any rotation between the coordinate systems.

The model is constructed by applying the Photometric Distance Law (1.1) twice: Firstly to calculate in a forward-step the Illuminance created by the source on the detector for a certain machine position, and secondly in a reverse-step to calculate the erroneous Luminous Intensity measurement reported by the goniometer for this Illuminance. The second step is already stated in equation (2.1). The incidence angle α can be assumed to be zero degrees for a detector aligned perpendicular to the center and this factor is subsequently left out.

The first step is more complex. To calculate the Illuminance $E(\phi,\theta)$, the geometry between source and detector for this specific measurement direction exemplified in Figure 3 needs to be known. Then it can be calculated with equation (3.1) from the source LID $I_{?}(C,\gamma)$ as follows:

$$E(\phi,\theta) = \frac{I_{?}(C,\gamma)}{\mathrm{r}'^2} \cdot cos(\alpha') \qquad (3.1)$$

The key to this geometry is to determine the detector position in the source coordinate system. In machine coordinates it is the point defined by the known goniometer direction and measurement distance $\boldsymbol{D_m} = (\phi,\theta,r)$. Similarly, the detector position in source coordinates is defined as $\boldsymbol{D_s} = (C,\gamma,r')$, which contains the actual measurement distance and direction.

To translate the detector position to the source coordinate system an intermediate cartesian representation is used, to move between coordinate systems. For this, functions for transformations between cartesian and spherical coordinates are defined in equation (3.2).

$$(\mathrm{X},\mathrm{Y},\mathrm{Z}) = t_{cart}(\Phi,\Theta,R) \qquad (\Phi,\Theta,R) = t_{sphere}(\mathrm{X},\mathrm{Y},\mathrm{Z})$$

$$t_{cart}\colon \begin{cases} \mathbb{R}^3 \to \mathbb{R}^3 \\ \mathrm{X} \mapsto R \cdot sin(\Theta) \cdot cos(\Phi) \\ \mathrm{Y} \mapsto R \cdot sin(\Theta) \cdot sin(\Phi) \\ \mathrm{Z} \mapsto R \cdot cos(\Theta) \end{cases} \qquad t_{sphere}\colon \begin{cases} \mathbb{R}^3 \to \mathbb{R}^3 \\ \Phi \mapsto atan2(\mathrm{Y},\mathrm{X}) \\ \Theta \mapsto arccos\left(\frac{Z}{\sqrt{\mathrm{X}^2+\mathrm{Y}^2+\mathrm{Z}^2}}\right) \\ R \mapsto \sqrt{\mathrm{X}^2+\mathrm{Y}^2+\mathrm{Z}^2} \end{cases} \tag{3.2}$$

Using the function t_{cart} (3.2) the detector position is converted to cartesian coordinates (3.3). Then this point is moved between the cartesian coordinate systems by subtracting the source translation vector $\mathbf{s_m}$ (3.4). Finally it is converted back to spherical coordinates in the source coordinate system using t_{sphere} in (3.5).

$$\mathbf{D_m} = t_{cart}(\boldsymbol{D_m}) \tag{3.3}$$

$$\mathbf{D_s} = \mathbf{D_m} - \mathbf{s_m} \tag{3.4}$$

$$\boldsymbol{D_s} = t_{sphere}(\mathbf{D_s}) \tag{3.5}$$

With (C,γ) and r' known, only the incidence angle α' is missing to calculate the Illuminance with equation (3.1). It is the angle between the normal vector of the detector surface and the incidence vector from the source location. This angle can be determined with equation (3.6). The cartesian detector positions in the machine and source coordinate system are interpreted as vectors $\mathbf{d}_{\square} = \mathbf{D_m}$ and $\mathbf{d}_{\square} = \mathbf{D_s}$, whose angle is calculated using the dot product.

$$cos(\alpha') = \frac{\mathbf{d_m} \cdot \mathbf{d_s}}{\|\mathbf{d_m}\| \cdot \|\mathbf{d_s}\|} \tag{3.6}$$

With all geometric quantities determined, equation (3.1) is inserted into (2.1). This yields the model for the goniometer measurement I_m given in (3.7), which is separated in the three different influence factors described in section 2.2:

$$I_m(C,\gamma,\mathbf{s_m}) = \underbrace{I_s(C,\gamma)}_{direction} \cdot \underbrace{\frac{r^2}{r'^2}}_{distance} \cdot \underbrace{cos(\alpha')}_{incidence} \tag{3.7}$$

While the other two components are wholly dependent on the source location, the directional component introduces an additional dependency for the LID of the source. The greater the LID differs between the assumed and actual direction, the greater the error.

4 Simulations for $\cos^n$ sources

Simulations are performed with LIDs constructed from a power of the cosine function (4.1), since many sources can be approximated well by cos^n terms [3].

$$I(C,\gamma) = 100\,\text{cd} \cdot cos^n(\gamma) \qquad (4.1)$$

The LID has a maximum Luminous Intensity of arbitrarily chosen 100 cd and decreases with the polar angle γ. For $n = 1$ the source has Lambertian characteristics. For higher n the LID gets increasingly collimated, which is suited to model luminaires with focusing optics. It has no dependency on the C-plane angle, making it symmetrical to the optical or z-axis.

Since all parts of the model from section 3 are invariant to scaling, this model can be used with relative units: All distances are expressed relative to the measurement distance r. This way the results can be generalized to different goniometer geometries. The goal is to investigate the deviation between the LID of the source and the simulated measurement result to find out how and how much the LID is distorted.

Which extent of translation is realistic for the PC is very dependent on the object and circumstances of a measurement. One way for the translation to become significant is prioritizing repeatability of the position rather than accuracy of the PC. An example would be a luminaire positioned with its light outlet plane in the machine center, as it is done for headlamps.

The extent of translation is also different for the particular axes. If the luminaire has focusing optics, its PC can be shifted considerably along the optical axis, even outside the housing dimensions. A translation of 1% of the measurement distance is chosen for the z-axis as a realistic estimate of what can be encountered. For a measurement distance of 10 m, this would equate a 10 cm offset.

Figure 5 shows a simulation of this translation for $n = 1$. An offset along the optical axis affects every C-plane the same. Because of this the effects of a positive and negative offset are combined in one diagram. The deviation is plotted in relative terms as a percentage of the source LID on the axis on the right. For a positive offset, as displayed in the C180 plane on the left side, the LID is reported ca. 2 % too high at $\gamma = 0°$. For increasing angles, the deviation is reduced and then becomes negative. In the outer region, where the source LID is small, the relative error takes on large values. For a negative offset the result is similar, but reversed.

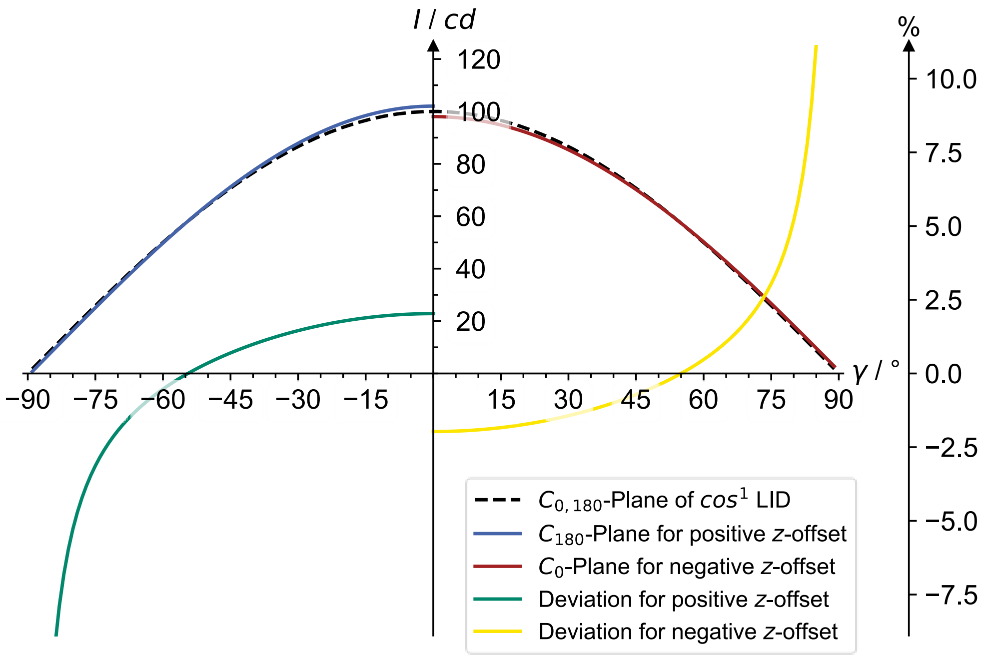

Figure 5 simulated LID measurement deviation for cos^1 source with z-axis offset

To get an understanding for the composition and origin of this deviation, Figure 6 shows the three different factors, that the error comprises. To compare the effect of the changed direction with the distance and incidence factors, the difference in Luminous Intensity between the assumed and actual measurement direction is expressed as a factor as well.

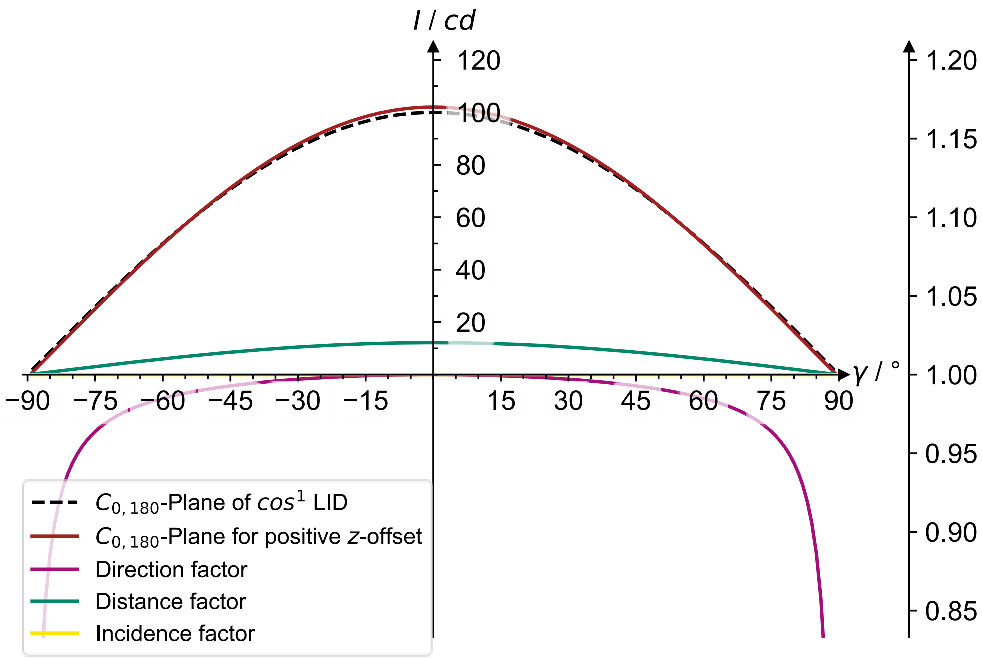

Figure 6 simulated LID measurement factors for cos^1 source with z-axis offset

The initial increase at $\gamma = 0°$ is caused exclusively by the shortened measurement distance. The difference in measurement distance reduces for steeper angles, while the direction becomes the dominating factor. The incidence factor is very close to one, having nearly no influence.

To examine the influence of the LID's gradient, the same geometry is simulated with the LID changed for $n = 100$, resulting in deviations as shown in Figure 7.

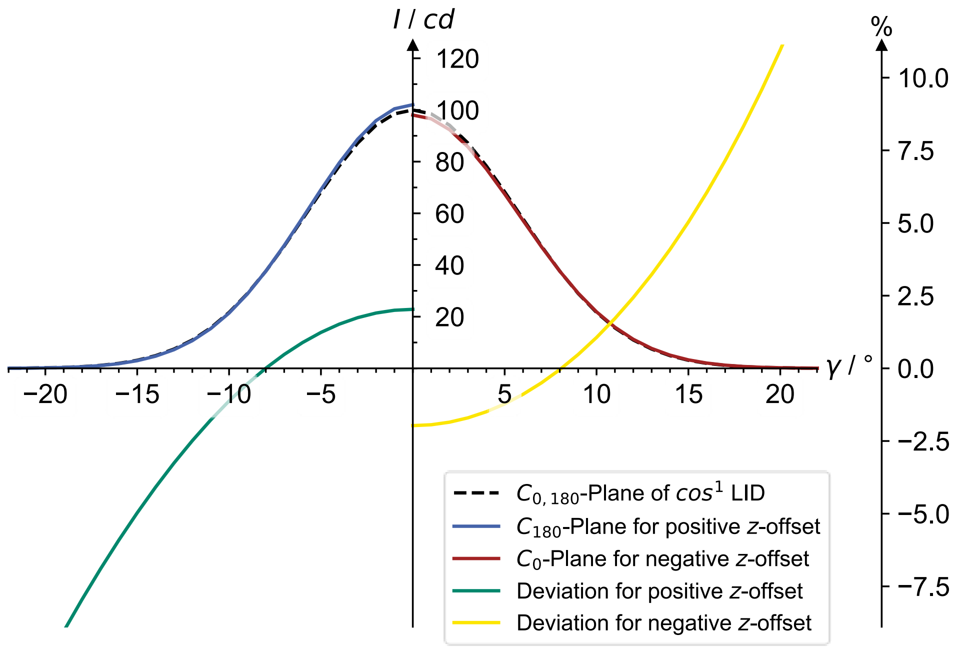

Figure 7 simulated LID measurement deviation for cos^{100}source with z-axis offset

The deviation for $\gamma = 0°$ is unchanged, since it does not depend on the gradient. For the angle range before the LID vanishes, the extent of the deviation is similar to the $n = 1$ case. The gradient of the LID and therefore the deviation for a certain angle is far greater, but the LID falls off fast enough, that this has no practical relevance.

The symmetry of the LID as simulated here, is normally also reflected in the construction of the luminaire, which makes it easier to position the object along the x- and y-axis. Any translation orthogonal to the optical axis is consequently less pronounced. For the simulation it is set an order of magnitude lower at 0.1% of the measurement distance.

A simulation for the Lambertian case is shown in Figure 4, displaying overall small relative deviations. In comparison, the deviations for a $n = 100$ source LID are much larger, as depicted in Figure 8. Because of the symmetrical LID it is sufficient to look at one of the perpendicular axes. The point source is translated along the x-axis and the effect observed in the C0 and C180 plane. For the shown angle range the deviation has a nearly linear dependency, reaching values upwards of 2 % for the outer angle regions, despite the smaller translation. At least for the active angle region, this kind of high gradient source is more susceptible to translations orthogonal to the optical axis.

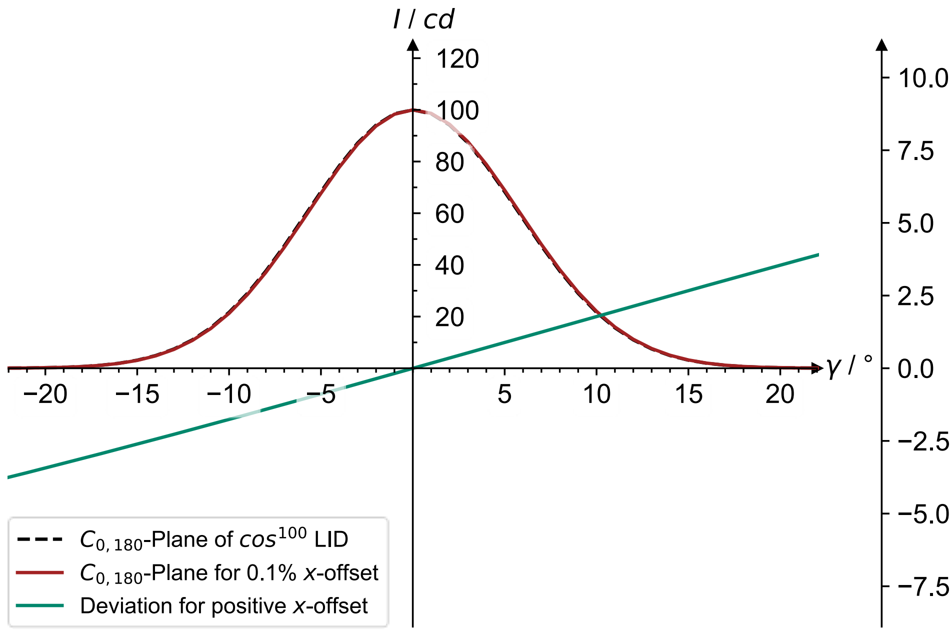

Figure 8 simulated LID measurement deviation for cos^{100}*source with* x*-axis offset*

Both the LID gradient and the amount of translation are compounding influences, since it is generally harder to estimate the PC for sources with focusing optics. One has to be especially aware of the potential influence of the PC when evaluating a LID for high polar angles, since these suffer from the largest relative deviations.

5 Uncertainty evaluation

The measurements that make up a LID are each afflicted with an uncertainty. It is an ongoing effort to model this uncertainty distribution, since most LID measurements currently lack an uncertainty evaluation entirely. The model created in section 3 is used to investigate the contribution to the measurement uncertainty brought about by an uncertain PC.

This is done via a Monte Carlo simulation [6]: The input parameters are modelled as uncertain and assigned a probability distribution. These distributions are then sampled many times, each time feeding them into the model and calculating the output. The large set of outcomes is then subjected to standard statistical analysis to determine the propagated uncertainty. This requires formulating a level of confidence in the position or PC of the object. This can be done by defining a region, in which the PC lies with a high certainty.

The direct result of an uncertain PC is an uncertain Luminous Intensity measurement for an uncertain direction, which is not easy to reason about. As modelled here the uncertainty of the direction is propagated to the uncertainty in Luminous Intensity by using knowledge about the source's LID.

A simulation is done for the case specified in section 4. The translations along the axes are modelled by normal distributions with an expectation of 0. For the z-axis the standard deviation is set to 0.5 % of the measurement distance, so that the relative expanded uncertainty is 1 % with a coverage factor of 2. The probability distribution of the translation along the orthogonal axes is modelled as a symmetric two-dimensional gaussian distribution with a relative expanded uncertainty of 0.1 %. The standard deviation along the separate axes then comes out to $\sqrt{2} \cdot 0.05$ %. The results are plotted in Figure 9. It shows the source LID and the overlaid expanded uncertainty of the simulated measurement. The expanded uncertainty is also plotted as a percentage relative to the source LID in yellow.

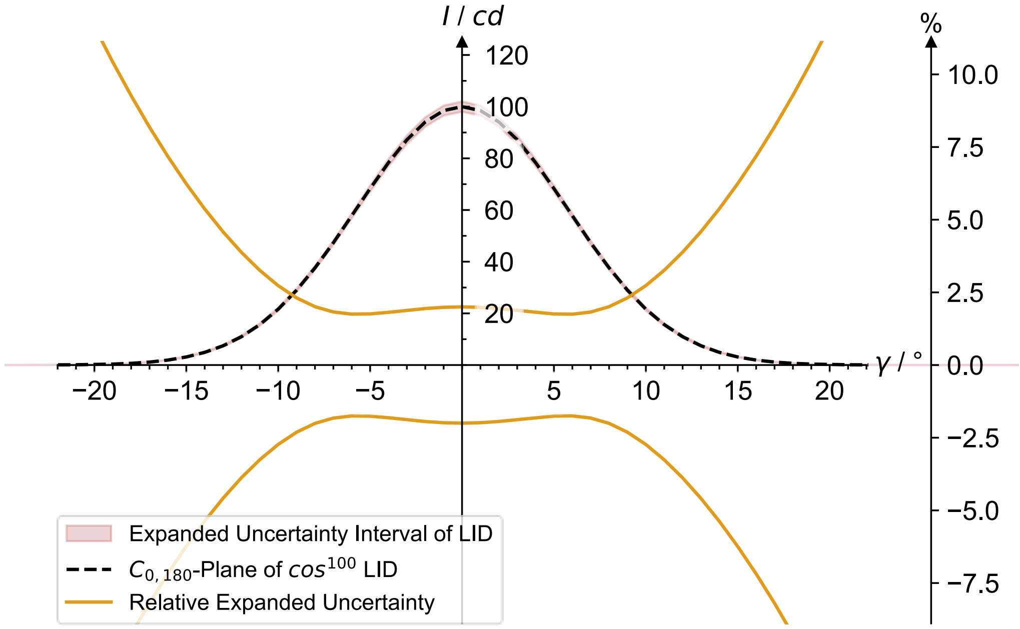

Figure 9 simulated LID measurement uncertainty for cos^{100} source

The resulting uncertainty distribution resembles a combination of the separate effects explored in section 4. The amount of uncertainty displayed in this example would be a dominating factor for most measurement setups. While the impact cannot be generalized from this example alone, it highlights the need to assess the uncertainty of the PC for any far field measurement.

6 Conclusion & Outlook

A model was formulated to investigate the impact of a translated PC and demonstrated, that it can be significant even for moderate translations. This model can also be used to correct a Luminous Intensity measurement according to equation (3.7), if the translation of the source is known. This would eliminate the positioning requirement.

The source could then be aligned to more repeatable points, feeding the PC location into the LID calculation.

Furthermore, it is shown, that the PC needs to be part of a LID uncertainty model. Integrating it would require rules and education on how to estimate the uncertainty of the PC. Otherwise there is a risk of underestimating its contribution. Another difficulty of this endeavour is the dependency of the model on the actual LID of the source, which is unknown. An approach to solving this could be to feed the measured LID as an approximate source LID back into the model for the uncertainty calculation.

The model only applies for goniometers with a constant detector distance. It could further be extended to capture far field goniometers with more complicated, not angle-constant geometries as the screen- or camera-based goniometer.

Ultimately the most sensible solution for handling the PC would involve measuring its location to correct for it. This would relieve the operator of the task of evaluating the PC or its uncertainty and drastically lower its uncertainty contribution. The necessary information could come from sparse near field measurements in the form of Luminance images of the source. A screen goniometer could offer another way of deriving the PC using overlapping screen regions, which contain Illuminance information for different distances.

7 References

[1] DIN EN 13032-1:2012-06, Licht und Beleuchtung- Messung und Darstellung photometrischer Daten von Lampen und Leuchten- Teil 1: Messung und Datenformat, DIN Media, Berlin, 2012.

[2] S. Wendel, S. Lück, and C. Neumann, “Constructing multiple focal points using rayfiles,” 10th Lux junior, Dörnfeld/Ilm: TU Ilmenau, 2011.

[3] V. Jacobs et al., “ANALYSES OF ERRORS ASSOCIATED WITH PHOTOMETRIC DISTANCE IN GONIOPHOTOMETRY,” 28th CIE SESSION, Manchester, 2015.

[4] M. Katona et al., “Systemanalyse eines bildgebenden LVK Messsystems mittels Monte Carlo Simulation,” 14th Lux junior, Dörnfeld/Ilm: TU Ilmenau, 2019.

[5] F. Gassmann et al., “Comparison of luminous intensity distributions,” Lighting Research & Technology, vol. 49, no. 1, pp. 62–83, Feb. 2017.

[6] Evaluation of measurement data — Supplement 1 to the “Guide to the expression of uncertainty in measurement” — Propagation of distributions using a Monte Carlo method, JCGM, 2008.